Atmos. Chem. Phys. Discuss., 10, 8963–8994, 2010
www.atmos-chem-phys-discuss.net/10/8963/2010/

Atmospheric Chemistry and Physics Discussions

The role of tropical deep convective clouds on temperature, water vapor, and dehydration in the tropical tropopause layer (TTL)

J. H. Chae[1,2], D. L. Wu[1], W. G. Read[1], and S. C. Sherwood[3]

[1]Jet propulsion Laboratory, California Institute of Technology, Pasadena, California, USA
[2]Joint Institute for Regional Earth System Science and Engineering University of California, Los Angeles, Los Angeles, California, USA
[3]Climate Change Research Centre, University of New South Wales, Sydney, Australia

Received: 23 March 2010 – Accepted: 28 March 2010 – Published: 7 April 2010

Correspondence to: J. H. Chae (junghyo.chae@aya.yale.edu)

Published by Copernicus Publications on behalf of the European Geosciences Union.

Abstract

Temperature and water vapor variations due to clouds in the TTL have been investigated using co-located MLS, CALISPO, and CloudSat data. Convective cooling occurs only up to cloud top heights, but there is warming above these heights in the TTL. Water vapor and ozone anomalies above cloud top heights support that the warming anomalies occur due to downward motion. Thicker clouds cause a greater magnitude of the temperature anomalies. Water vapor of the environment below cloud tops can either increase or decrease, depending on the cloud top height. The critical factor, which divides these different water vapor variations below cloud tops, is the relative humidity. Clouds hydrate the environment below 16 km, where the air after mixing between cloud and the environmental air does not reach saturation, but clouds dehydrate above 16 km, due to the supersaturation because of the larger temperature drop and the high initial relative humidity. Water vapor above cloud tops has negative anomalies compared to clear skies and suggests another dehydration mechanism.

1 Introduction

The tropical tropopause is important for understanding the future state of our climate system because tropospheric air, which includes water vapor and other trace gases, enters the stratosphere preferentially through this layer (Brewer, 1949). The tropical tropopause is not a fixed material surface but rather a mixed layer, with both tropospheric and stratospheric characteristics; it is termed the tropical tropopause layer (TTL, Fueglistaler et al., 2009). The bottom of the TTL, located near 15 km, is usually defined as the level of zero net radiative heating where the net radiative heating changes from cooling to heating. The air above this level tends to rise, owing to the wave-driving stratospheric Brewer-Dobson circulation, and it eventually enters the stratosphere, whereas the air below this level sinks owing to convective circulations. The top of the TTL, located at a height of ∼18 km, is the maximum height of

ACPD
10, 8963–8994, 2010

The role of tropical deep convective clouds

J. H. Chae et al.

overshooting convection. Therefore, the bottom of the TTL is the lowest level where stratospheric features can be found, whereas the top of the TTL is the highest level where tropospheric features are apparent.

One of most important unsolved questions is the water vapor transport process from the troposphere to the stratosphere, especially because the analysis of recent decadal records shows that water vapor in the stratosphere is increasing. Water vapor is a greenhouse gas, and long-lived stratospheric water vapor can affect the global energy budget, and it has been shown that increasing water vapor in the stratosphere cools the stratosphere but heats the troposphere (Forster and Shine, 1999; Smith et al., 2001). It is commonly agreed that transport and dehydration processes occur within the TTL, but there is no concrete hypothesis on the manner in which water vapor is transported from the troposphere to the stratosphere (e.g., Read et al., 2008). Two hypotheses have been considered. “Cold trap dehydration” is the hypothesis that assumes a slow ascent by large-scale freeze-drying through a particularly low temperature area over the western Pacific. Lagrangian trajectory studies (Fueglistaler et al., 2005) and the frequent existence of in-situ thin cirrus clouds near the TTL (Jensen et al., 1996) support this hypothesis. The other hypothesis is based on “convective dehydration”, which occurs mainly due to the effects of deep overshooting convection (Sherwood and Dessler, 2001).

However, neither of these hypotheses fully explains the process of water vapor entry into the tropical stratosphere. Some modeling studies show that overshooting convection, penetrating the cold point, hydrates the lower stratosphere instead of dehydrating it because these overshooting clouds can contain cloud ice, which can re-evaporate under the warmer temperatures (Jensen et al., 2007; Corti et al., 2008). On the other hand, it is observed that HDO, the heavy water isotope, changes very little with height in the TTL. This can not be explained by the slow ascent dehydration process (Kuang et al., 2003; Dessler et al., 2007; Read et al., 2008).

It has long been recognized the upper troposphere in the western Pacific is the coldest longitudinally (Arakawa, 1950). This upper tropospheric cold region has links to tropical deep convection because the western Pacific is a frequent deep convection area. However, the mechanism of the TTL cooling, in relation to tropical deep convection, has been debated and there are several hypotheses centered on the following: convective detrainment and diabatic turbulent mixing with the environment (Sherwood, 2000; Sherwood et al., 2003; Kuang and Bretherton, 2004), convectively generated waves (Tsuda et al., 1994; Zhou and Holton, 2002; Randel and Wu, 2005), radiative cooling by reduction in longwave heating (Webster and Stephens, 1980; Norton, 2001), and intrinsic responses to convective heating in free troposphere, which is followed by divergence, ascent and adiabatic cooling (Holloway and Neelin, 2007).

Even though the temperature and water vapor in the TTL are closely linked to tropical convective activity, the manner in which clouds influence these variables is still uncertain because there are few datasets that contain collocated cloud and environmental thermodynamical information. Additionally, previous cloud top height measurements using the brightness temperature technique had low biases (Sherwood et al., 2004), and therefore might have missed some important features. In this study, we use high-resolution satellite data to identify the convective influence on temperature and water vapor.

We focus especially on cloud top height in order to investigate how cloud ice influences environmental temperature and water vapor variations. We hypothesize that cloud top height is one of the most important factors that influences environmental temperature and water vapor in the TTL, because the thermodynamic condition of cloudy air uplifted into the TTL is much different from that of the environment.

The data and methods used in this study are described in the next section. Section 3 deals with cloud top heights obtained from CALIPSO and CloudSat, and how these values differ from previous satellite data. Section 4 shows the relationships between cloud top heights and environmental temperature, water vapor, and ozone. Conclusions and discussion are presented in Sect. 5.

2 Data

We use MLS v2.2 temperature, water vapor, and ozone datasets, which have been validated by Read et al. (2007), Schwartz et al. (2008), and Froidevaux et al. (2008). MLS temperatures have been modified by offset factors obtained by comparison with GPS data at each pressure level. MLS data have a vertical resolution of 3–4 km, and a horizontal resolution of approximately 7 km across track and 200–300 km along track.

Level 1 CALIPSO backscattering data are used for cloud information. We use only the nighttime dataset because of excessive noise during the daytime (see Wu et al., 2010). Cloud top height is the most important variable in our analysis, and CALIPSO is the best source of this information. CloudSat is used to determine thick and thin clouds because CALISPO backscattering is quickly attenuated in clouds.

Aura, CALIPSO, and CloudSat are different satellites, and there are only limited time periods when CALIPSO measurements are close to MLS within the MLS horizontal resolution, though all these are in the A-train (Stephens et al., 2002) in the same orbit and pass a given latitude within a short time period (7 min). Here we used data over a nine-month period from May 2008 to January 2009, when the orbits of MLS and CALIPSO were within 10 km of each other at the equator. Only tropical data (15° S to 15° N) are used because we are mainly interested in the TTL.

We attempted to divide cloud types into three categories: thick, thin and multi-layered clouds, because these cloud types have different radiative heating effects. Thin clouds correspond to isolated thin cirrus clouds which cannot be detected by CloudSat, whose thicknesses are less than 3 km, and whose maximum backscatter is less than 0.0005 km^{-1} sr^{-1} from the CALIPSO data. Thick clouds are defined to be at least three km thick vertically, and CloudSat ice water content (IWC) greater than 2 mg/m^3 in the overlapping region. We categorize clouds as multi-layered clouds if there are other clouds present, with top heights greater than 10 km, beneath the thin cirrus clouds.

ACPD
10, 8963–8994, 2010

3 Distribution of cloud tops

Figure 1 shows the zonal distribution of cloud top height frequency averaged over the period from May 2008 to January 2009. In Fig. 1a, we see a prominent cloud top heights mode between 14 and 17 km, and three longitudinal areas (Africa, western Pacific, and Central America), contain frequent thick convective clouds (Fig. 1b). Multi-layered cloud frequency is similar to thick cloud frequency because the upper thin cirrus clouds above lower high-topped clouds are associated with deep convective clouds (Fig. 1c). On the other hand, isolated thin cirrus clouds (in-situ cirrus) in Fig. 1d show little longitudinal dependence. Our analysis indicates that half of the cirrus clouds have underlying deep convection or are associated with other thin clouds (19.4%), and the other half are isolated single layer cirrus clouds (20.6%). This analysis is consistent with the result of a previous study (McFarquhar et al., 2000).

Lidar observations from CALIPSO are very sensitive to optically thin clouds, and the cloud top heights inferred from these observations are much higher than other observations. Figure 2 shows one example of different cloud top heights obtained from two different satellite instruments. The maximum peak height of cloud tops from CALIPSO-CloudSat is close to 16.5 km, whereas that from the Multi-angle Imaging SpectroRadiometer (MISR) is close to 13 km. This height difference of approximately 3–4 km between the peaks from the observations from two different satellites is not surprising because MISR cannot detect very thin cirrus clouds, and even thin overlying clouds (optical depth of as high as five) can be missed when there are thicker clouds below them (Marchand et al., 2007). However, this peak height difference still exists when we compare thick clouds only from CALIPSO-CloudSat to those from MISR data. This indicates that CALIPSO-CloudSat can detect cloud tops much higher than MISR can, even though they observe the same clouds. Other previous studies have also shown that CALIPSO cloud top heights are 3–4 km higher than MODIS or AIRS heights in tropical deep convective clouds (Holz et al., 2008; Wu et al., 2009).

ACPD

10, 8963–8994, 2010

Title Page
Abstract Introduction
Conclusions References
Tables Figures
◀| |▶
◀ ▶
Back Close
Full Screen / Esc
Printer-friendly Version
Interactive Discussion

4 Results

4.1 Cloud top height vs. temperature

Figure 3 shows the time mean zonal and vertical temperature anomaly structure (deviations from the zonal mean) obtained by removing the annual cycle at each altitude. There are warm anomalies up to 13 km, followed by colder temperatures near the TTL over the western Pacific where strong deep convection frequently occurs. In the eastern Pacific, in the descending region of the Walker circulation, there are warm anomalies above cold anomalies in the troposphere. These zonal temperature anomalies are consistent with the findings of previous studies (Randel et al., 2003; Randel and Wu, 2005; Gettelman and Birner 2007; Fueglistaler et al., 2009). These zonal temperature anomalies are also sustained in a clear sky because of the difference between the radiative relaxation time and cloud lifetime scales (Fig. 3b). The temperature anomalies induced by clouds can remain in a clear sky due to the relatively long radiative relaxation time, though it depends on the perturbation wavelength. The radiative relaxation time scale in the TTL is approximately 30–120 days (Hartmann et al., 2001), which is longer than cloud lifetimes (typically 1–2 days).

To see the effect of an individual convective event on the local environmental temperature, we investigated temperature anomalies from local (latitude-longitude bin; 5° by 5°) clear sky mean temperatures rather than from the zonal mean. When there were no clear skies (e.g. Western Pacific area), we used the average value of the nearest clear sky mean temperature. Figure 4a shows the temperature anomalies used for a cloudy condition in which there are clouds with tops higher than 10 km. The right-side figure shows the zonal average of each cloud type with height. Any local space in Fig. 4a can include both conditions, i.e., at times above cloud top and below at other times (14–18 km following Fig. 4b and c). Nevertheless, Fig. 4a shows that there are cold anomalies below 16 km, the level which is usually below the cloud tops, but there are warm anomalies above the cold anomalies, mostly above the cloud tops. There is little longitudinal variation except that the temperature anomaly tilts eastward with

ACPD
10, 8963–8994, 2010

Title Page
Abstract Introduction
Conclusions References
Tables Figures
◀◀ ▶▶
◀ ▶
Back Close
Full Screen / Esc
Printer-friendly Version
Interactive Discussion

height over two longitudinal bands. One is from the Indian Ocean to the west Pacific and the other is from the eastern Pacific to Central America. This eastward tilt with height agrees well with the maximum cloud top occurrence (see Fig. 1).

Figure 4b and c shows in detail how clouds influence the environmental temperature above and below cloud tops. Temperature data only from locations at least 1.5 km above cloud tops are used in Fig. 4b. For investigation below cloud tops, we used reference levels, which should be below cloud top height but not lower than 3 km below cloud top (Fig. 4c). These two figures show that the temperature anomalies have opposite signs, according to the reference level relative to the cloud top height. Figure 4b and 4 shows warm anomalies above the cloud and cold anomalies below the cloud top level in the TTL.

It should be noted that all satellite-derived temperatures inside clouds, including those obtained from MLS, are not reliable, and indicate excessively cold conditions. In Fig. 4c, cold anomalies below cloud tops are ubiquitous, even though the cloud top height is below 14 km, which is usually considered the Level of Neutral Buoyancy (LNB). The cloudy air should be warmer than the environment up to the LNB because of the release of latent heat, and a warm temperature anomaly should be seen. The cold anomalies below 14 km in Fig. 4b might suggest that warm anomalies are needed below 14 km in Fig. 4c as the opposite manner of behavior. According to following analyses of water vapor and ozone, when the environmental levels are above cloud top, the anomalies below 14 km also show the opposite sign of that above 14 km. In this study, we do not consider the level below 14 km deeply because we mainly focus on the TTL. Even though the temperature inside the cloud is very uncertain, to qualitatively explain the cold temperature near the cold point over the western Pacific, cooling occurs below cloud top in the TTL because there are always warm anomalies above the clouds.

Figure 5 shows the temperature anomalies at the height relative to cloud top. It is clear that a warm anomaly occurs above the cloud top and a cold anomaly below it, and there is little longitudinal variation though there are very small cold anomalies far above the cloud top in some longitudinal areas (Fig. 5a). There is longitudinal variation far below the cloud top: cooling is deeper over frequent deep convective areas and the warm anomalies are apparent below cold anomalies especially over weaker convecting regions (e.g., the eastern Pacific). Figure 5b shows zonal averages segregated according to cloud types. The magnitudes of the anomalies are greatest in thick clouds, but the overall features are the same for different cloud types. In thin clouds, the warm anomaly occurs below three km from the cloud top due to their three km thickness definition.

The cooling anomalies below cloud tops occur in all cloud types, though their magnitudes are different. This indicates that the radiative heating term is not big enough to determine the local temperature because our result is contrary to the findings of many previous studies, which have shown that there is local net radiative heating in thin cirrus clouds, though there is net radiative cooling in thick cloud tops and in cirrus clouds having thick clouds below them (Rosenfield et al., 1998; McFarquhar et al., 2000; Hartmann et al., 2001). This radiative heating contributes only to the reduction of the magnitude of the cooling in thin clouds. The sign change from a cooling to a warming anomaly strongly depends on cloud top height. This indicates that direct turbulent mixing between the cold cloudy air and the environment is the predominant process for cooling.

The warming mechanism for the region above the cloud is not clear. There are several hypotheses for this possibility. One of them invokes the Kelvin wave generated by convective diabatic cooling in the top levels or convective heating in the free troposphere. The cold anomaly above the warm anomaly in Fig. 4b looks like a wave feature which would support this theory. The other hypothesis involves the direct response to cooling below the cloud top because cooling shrinks the local thickness and there should be a downward motion above the cooling.

In addition to measuring uncertainty described above, we should also be careful about the quantitative analysis of warming anomalies above the cloud tops, because our analysis uses local clear sky temperature as the background, and the clear sky temperature is not the same in all domains, due to the longer radiative relaxation time scale versus cloud lifetime, as shown in Fig. 3b. For example, temperature anomalies in clear skies over frequent convective areas still persist after clouds are dissipated, although the magnitudes of convective cooling below and warming above the cloud top are reduced with time. The difference in the radiative relaxation time scale with height also explains why the maximum cold anomaly from the zonal mean temperature occurs near the cold point, even though the maximum occurrence of cloud tops is 1–2 km below the cold point.

4.2 Cloud top height vs. water vapor

Before we investigate the relationship between the cloud top height and environmental water vapor, we examine the relation between temperature and water vapor using MLS data. Figure 6 shows the contours of temperature versus water vapor frequency from MLS at four pressure levels (82, 100, 121, and 146 hPa), using data obtained from June to August 2008 (the boreal summer) and December 2008 to January 2009 (the boreal winter). We selected two different seasons because thermodynamic variables in the TTL have a strong annual cycle (Resonlof, 1995; Reid and Gage, 1996; Chae and Sherwood, 2007), caused by large scale wave-driven stratospheric circulation, called the Brewer-Dobson circulation (Brewer, 1949; Yulaeva, 1994). The coldest temperature, for example, is shown near 82 hPa in the boreal winter but near 100 hPa in the boreal summer, and the water vapor mixing ratio in summer is ~2 ppmv higher than in winter at 100 hPa. The dash-dot line indicates the saturated mixing ratio and therefore the overlapping areas, located at the lower right side of the figure, are in supersaturated conditions or overestimated values caused by contamination due to ice particles (clouds). The 82 hPa level in summer, which is in the lower stratosphere above the cold point, is not saturated because there are few clouds present and the relative humidity is low because of the increase in temperature.

MLS data show an interesting relation between temperature and water vapor (Fig. 6). At 121 hPa and below, the variability of water vapor is relatively large compared to that of temperature, whereas temperature variability is very high at 100 hPa and above.

ACPD
10, 8963–8994, 2010

The level between 100 and 121 hPa is a transition layer. Water vapor is negatively correlated with temperature at 146 and 121 hPa (lower TTL). The positive correlation at 100 and 82 hPa (upper TTL) is consistent with the findings of previous studies, in which temperature was found to control water vapor at 100 hPa (Holton and Gettelman, 2001; Read et al., 2004). This demonstrates to us that the physical mechanisms which determine temperature and water vapor at these two levels are different from each other.

Water vapor is analyzed in a way similar to temperature in Fig. 4 (Fig. 7). Figure 7a shows the cloudy sky water vapor anomalies from local clear sky water vapor, which increase below 16 km in cloudy skies but decrease near the cold point. As shown in the temperature analysis, the altitude from 14 to 18 km can be either above or below the cloud top height. Therefore, we have to be careful to infer possible cloud effects on water vapor in the TTL. Water vapor anomalies above (Fig. 7b) and below the cloud top height (Fig. 7c) are also shown in the same way as the temperature anomalies in Fig. 4.

In the environment below the cloud top, water vapor can either increase or decrease, depending on the height (Fig. 7c). Clouds itself always humidify the environment if cloud tops are at 16 km or lower, but dehydrate if the cloud tops can are higher than 16 km. This can be explained by examining the relative humidity with respect to ice, as shown in Fig. 8. The temperature of the mixed air is always cooled as shown in Fig. 4c, and the relative humidity increases with height below the cloud tops in the TTL. The air is still below saturation below 16 km (or slightly super saturated near 16 km), and therefore clouds can supply water vapor to the environment at those heights. The environment becomes supersaturated above 16 km, however, and therefore clouds cannot supply water vapor to the environment at those heights. On the contrary, preexisting water vapor before mixing has to be condensed out, and this generates cirrus clouds.

On the other hand, water vapor variations above the cloud top are totally different from those below the cloud top. Water vapor has negative anomalies above the cloud top if the cloud has penetrated to approximately 14 km (near the LNB). The magnitude

ACPD
10, 8963–8994, 2010

of the decreasing of water vapor does not depend on cloud top height but rather on the reference altitude. The bigger decrease of water vapor is at the lower altitudes in the TTL.

4.3 Cloud top height vs. ozone

Ozone can be effectively used as a tracer to understand the physics of the TTL, including for making estimates of cloud top heights and understanding troposphere-stratosphere exchanges (e.g., Folkins et al., 1999). Ozone is vertically well mixed and does not show significant vertical gradients in the troposphere, except that it has a local minimum near 200 hPa in the tropics which is considered to be a level of convective detrainment (see Fueglistaler et al., 2009). However, ozone begins to increase within a transition zone between 14 and 17 km in which the chemical characteristics of the stratosphere begin to develop.

Figure 9 shows ozone anomalies from local clear sky ozone concentrations, determined by the same method of analysis as that used for Figs. 4 and 7. Cloudy sky ozone in the cloudy sky increases above 16 km and below 12 km, but decreases between these two levels (Fig. 9a). When we consider the variations of ozone concentrations above and below cloud top height, similar to temperature and water vapor, it is clear that ozone increases above the cloud top but decreases below the cloud top if the reference height is above 12 km (Fig. 9b and c). The increasing ozone anomalies below 12 km are not a surprising result. Convective upwelling and mixing occur below the cloud top, and the local minimum of ozone is around 12 km (200 hPa). Therefore, convective upwelling induces an increase below 12 km but a decrease above that level.

An interesting feature is the increase of ozone above the cloud top height. If we assume that chemical ozone production and sinking are both the same in the cloudy and the clear skies, the ozone increase should be the result of adiabatic processing. It indicates that the air above the cloud top has a downward motion because ozone concentrations increase with height in the TTL. This agrees well with temperature variations (warm anomalies) and water vapor variations (negative anomalies up to the cold point where water vapor has a local minimum).

5 Conclusions and discussion

In this study, we investigated temperature and water vapor variations due to clouds in the TTL using co-located MLS, CALISPO, and CloudSat datasets. The new lidar measurement of cloud top heights and corresponding environmental variables from A-train satellites in the same orbit enable us to compare variables between each cloud and clear event in the TTL. CALIPSO data of the tropical deep convection and thin cirrus clouds (above 10 km) show the cloud top heights to be 2–4 km higher than those observed from other previous instruments. The peak of cloud top height frequency of CALIPSO is near 15 km, which is far above the LNB, and indicates that tropical deep convective clouds and detrained anvil and cirrus clouds overshoot mostly.

The relation between clouds and environmental temperature in the TTL clearly shows that convective cooling occurs only up to cloud top heights, with warming above these heights. These temperature anomalies do not depend on longitude. Thicker clouds are associated with a greater magnitude of the temperature anomalies. The magnitude of temperature anomalies may also depend on cloud top height in the TTL for overshooting clouds, because the temperature of an overshooting cloud get colder with height to a greater extent than the environment (Fig. 10). However, we do not investigate temperature anomalies quantitatively in this study because temperature measurements inside clouds are difficult and associated with large uncertainties. Additionally, a long radiative relaxation time induces a memory effect in which the clear-sky temperature is influenced by previous convective activity. This reduces the temperature anomalies near the cold point over areas of frequently convective activity such as the western Pacific.

The cooling anomalies below the cloud top height exist in clouds of all types, including isolated thin cirrus clouds, which radiatively heat local areas. Radiative cooling by water vapor can also contribute to a temperature drop, at least up to 16 km, because clouds humidify the environment, but it should be the opposite above 16 km because clouds dehydrate at these levels. However, we could not find any heating effect below cloud tops when they were above 16 km. Therefore, radiative cooling by water vapor cannot be a dominant cooling factor. Kelvin waves generated by convective heating in the free troposphere can be also considered as one of the cooling factors, but this cannot fully explain why cooling is limited to below cloud top heights. This indicates that other cooling factors should exist. Another hypothesis for the convective cooling effect is based on turbulent mixing between cold cloudy air and warm environmental air, because overshooting clouds that penetrate the LNB in the TTL are always colder than the environment (see Fig. 10).

The warming anomalies above cloud top heights provide interesting results. These warming anomalies occur above all cloud types but the magnitude of warming seems to be proportional to the cooling anomalies below cloud top heights, which means that there is more warming and cooling in thick clouds than thin clouds above and below cloud tops, respectively.

We performed a simple estimate of anomalies (cloudy minus clear) of water vapor and ozone due to a vertical displacement, giving the observed change in temperature. If air moves adiabatically, we can estimate the water vapor and ozone anomalies by following equation.

$$\Delta A \approx \left(\Delta\theta \bigg/ \frac{d\theta}{dz}\right)\frac{dq}{dz} \tag{1}$$

Here, θ is potential temperature, and A is either water vapor (q) or ozone (O_3). We used nine months average for observed variables. Table 1 shows an example at 15.6 km. The variation of all three variables, having the same sign as each gradient variation, concludes air descent. Additionally, the observed water vapor and ozone anomalies are two or three times larger than expectations based on temperature. This means that the temperature change is reduced by mixing and cooling.

According to above calculation, and corresponding water vapor (Fig. 7b) and ozone (Fig. 9b) anomalies, these warming anomalies are due to downward motion. Sherwood (2000) investigated the downward motion in the lower stratosphere over the western Pacific. However, because of the poor resolution of the cloud top data, he thought that there were cooling anomalies rather than warming anomalies above the cloud tops. Therefore, he argued that the downward motion and cooling is due to mixing and rearrangement between colder overshooting convective clouds and the warmer environment (see Sherwood and Dessler, 2001). However, warm anomalies instead of cool anomalies above cloud tops do not indicate mixing between clouds and environmental air, but rather the response of mixing between downward air and pre-existed air.

The mechanism of warming and downward motion is not clear and can be explained by several different hypotheses. The most acceptable theory is the one related to the direct response of cooling by clouds. The diabatic cooling near the top area of a cloud shrinks its thickness, and a separate downward motion of air is required above this cooling level. On the opposite side, we can infer that the downward motion and warming are part of the Kelvin wave, and this wave feature affects cloud top heights. Several previous studies have shown that some isolated thin cirrus clouds are generated by Kelvin wave activity (Boehm and Verlinde, 2000; Immler et al., 2008). However, there is no evidence that stratospheric features including Kelvin waves can affect the cloud top height of deep convective clouds, and therefore Kelvin wave, itself, cannot fully explain temperature anomalies above and below cloud tops.

Water vapor variations due to clouds are also divided into regions above and below cloud top heights. Environmental water vapor of below cloud tops can either increase or decrease. The critical factor, which divides these different water vapor variations below cloud tops, is the relative humidity. Clouds hydrate the environment below 16 km, where the relative humidity after mixing between cloud and the environmental air does not reach saturation, but clouds dehydrate above 16 km because air there is supersaturated because of the bigger temperature drop and the high initial relative humidity.

Water vapor variations combined with temperature changes above cloud tops suggest another dehydration mechanism. Figure 11 shows a schematic of the dehydration processing above the cloud top height. Tropical convection penetrating the LNB cools the environment below cloud top but warm the environment above cloud top and cause air to descend. The descending air parcels contain less water vapor than the environment. If they mix with the ambient air, they dehydrate these levels, and eventually the mixed dry air parcels are horizontally advected from the convective areas and enter the stratosphere by Brewer-Dobson circulation.

In this study, because of the limitation of satellite data, we do not investigate temperature anomalies of pre- and post-convective activities, which are important for understanding the impact of the Kelvin waves on temperatures in the TTL. Therefore, further studies are required for understanding the factors in detail that induce temperature variations near cloud top in the TTL.

Acknowledgements. We would like to thank T. Kubar for help and advice and M. Schwartz for helpful discussions on MLS instrument. This research was funded by NASA grant 443983-LI-79043.

References

Arakawa, H.: Analysis of the tropopause and the stratospheric field of temperature of a mature typhoon, Pap. Meteorol. Geophys., 2, 1–5, 1950.

Boehm, M. and Verlinde, J.: Stratospheric influence on upper tropospheric tropical cirrus, Geophys. Res. Lett., 27, 3209–3212, 2000.

Brewer, A. W.: Evidence for a world circulation provided by the measurements of helium and water vapor distribution in the stratosphere, Q. J. Roy. Meteorol. Soc., 75, 351–363, 1949.

Chae, J. H. and Sherwood, S. C.: Annual temperature cycle of the tropical tropopause: A simple model study, J. Geophys. Res., 112, D19111, doi:10.1029/2006JD007956, 2007.

Corti, T., Luo, B. P., de Reus, M., Brunner, D., Cairo, F., Mahoney, M. J., Martucci, G., Matthey, R., Mitev, V., dos Santos, F. H., Schiller, C., Shur, G., Sitnikov, N. M., Spelten, N., Vössing, H. J., Borrmann, S., and Peter, T.: Unprecedented evidence for deep convection hydrating the tropical stratosphere, Geophys. Res. Lett., 35, L10810, doi:10.1029/2008GL033641, 2008.

Dessler, A. E., Hanisco, T. F., and Fueglistaler, S.: Effects of Convective ice lofting

on H_2O and HDO in the tropical tropopause layer, J. Geophys. Res., 112, D18309, doi:10.1029/2007JD008609, 2007.
Folkins, I., Loewenstein, M., Podolske, J., Oltmans, S. J., and Proffit, M.: A barrier to vertical mixing at 14 km in the tropics: Evidence from ozonesondes and aircraft measurements, J. Geophys. Res., 104(D18), 22095–22102, 1999.
Forster, P. M. de F. and Shine, K. P.: Stratospheric water vapour changes as a possible contributor to observed stratospheric cooling, Geophys. Res. Lett., 26, 3309–3312, 1999.
Froidevaux, L., Jiang, Y. B., Lambert, A., Livesey, N. J., Read, W. G., Waters, J. W., Fuller, R. A., Marcy, T. P., Popp, P. J., Gao, R. S., Fahey, D. W., Jucks, K. W., Stachnik, R. A., Toon, G. C., Christensen, L. E., Webster, C. R., Bernath, P. F., Boone, C. D., Walker, K. A., Pumphrey, H. C., Harwood, R. S., Manney, G. L., Schwartz, M. J., Daffer, W. H., Drouin, B. J., Cofield, R. E., Cuddy, D. T., Jarnot, R. F., Knosp, B. W., Perun, V. S., Snyder, W. V., Stek, P. C., Thurstans, R. P., and Wagner, P. A.: Validation of Aura Microwave Limb Sounder stratospheric ozone measurements, J. Geophys. Res., 113, D15S20, doi:10.1029/2007JD008771, 2008.
Fueglistaler, S., Bonazzola, M., Haynes, P. H., and Peter, T.: Stratospheric water vapor predicted from the Lagrangian temperature history of air entering the stratosphere in the tropics, J. Geophys. Res., 110, D08107, doi:10.1029/2004JD005516, 2005.
Fueglistaler, S., Dessler, A. E., Dunkerton, T. J., Folkins, I., Fu, Q., and Mote, P. W.: Tropical tropopause layer, Rev. Geophys., 47, RG1004, doi:10.1029/2008RG000267, 2009.
Gettelman, A. and Birner, T.: Insights into Tropical Tropopause Layer processes using global models, J. Geophys. Res., 112, D23104, doi:10.1029/2007JD008945, 2007.
Hartmann, D. L., Holton, J. R., and Fu, Q.: The heat balance of the tropical tropopause, cirrus, and stratospheric dehydration, Geophys. Res. Lett., 28, 1969–1972, 2001.
Holloway, C. E. and Neelin, J. D.: The convective cold top and quasi equilibrium, J. Atmos. Sci., 64, 1467–1487, 2007.
Holton, J. R. and Gettelman, A.: Horizontal transport and the dehydration of the stratosphere, Geophys. Res. Lett., 28, 2799–2802, 2001.
Holz, R. E., Ackerman, S. A., Nagle, F. W., Frey, R., Dutcher, S., Kuehn, R. E., Vaughan, M. A., and Baum, B.: Global Moderate Resolution Imaging Spectroradiometer (MODIS) cloud detection and height evaluation using CALIOP, J. Geophys. Res., 113, D00A19, doi:10.1029/2008JD009837, 2008.
Immler, F., Krüger, K., Fujiwara, M., Verver, G., Rex, M., and Schrems, O.: Correlation between equatorial Kelvin waves and the occurrence of extremely thin ice clouds at the tropical

tropopause, Atmos. Chem. Phys., 8, 4019–4026, 2008, http://www.atmos-chem-phys.net/8/4019/2008/.

Jensen, E. J., Toon, O. B., Selkirk, H. B., Spinhirne, J. D., and Schoeberl, M. R.: On the formation and persistence of subvisible cirrus clouds near the tropical tropopause, J. Geophys. Res., 101, 21361–21375, 1996.

Jensen, E. J., Ackerman, S. A., and Smith, J. A.: Can overshooting convection dehydrate the tropical tropopause layer?, J. Geophys. Res., 112, D11209, doi:10.1029/2006JD007943, 2007.

Kuang, Z., Toon, G. C., Wennberg, P. O., and Yung, Y. L.: Measured HDO/H_2O ratio across the tropical tropopause, Geophys. Res. Lett., 30(7), 1372, doi:10.1029/2003GL017023, 2003.

Kuang, Z. and Bretherton, C. S.: Convective influence on the heat budget of the tropical tropopause layer: A cloud-resolving model study, J. Atmos. Sci., 61, 2919–2927, 2004.

Marchand, R. T., Ackerman, T. P., and Moroney, C.: An assessment of Multiangle Imaging Spectroradiometer (MISR) stereo-derived cloud top heights and cloud top winds using ground-based radar, lidar, and microwave radiometers, J. Geophys. Res., 112, D06204, doi:10.1029/2006JD007091, 2007.

McFarquhar, G. M., Heymsfield, A. J., Spinhirne, J., and Hart, B.: Thin and subvisual tropopause tropical cirrus: observations and radiative impacts, J. Atmos. Sci., 57, 1841–1853, 2000.

Norton, W. A.: Longwave heating of the tropical lower stratosphere, Geophys. Res. Lett., 28, 3653–3656, 2001.

Randel, W. J., Wu, F., and Rivera Ros, W.: Thermal variability of the tropical tropopause region derived from GPS/MET observations, J. Geophys. Res., 108(D1), 4024, doi:10.1029/2002JD002595, 2003.

Randel, W. J. and Wu, F.: Kelvin wave variability near the equatorial tropopause observed in GPS radio occultation measurements, J. Geophys. Res., 110, D03102, doi:10.1029/2004JD005006, 2005.

Read, W. G., Wu, D. L., Waters, J. W., and Pumphrey, H. C.: A new 137–56 hPa water vapor product from the UARS Microwave Limb Sounder, J. Geophys. Res., 109, D06111, doi:10.1029/2003JD004366, 2004.

Read, W. G., Lambert, A., Bacmeister, J., Cofield, R. E., Christensen, L. E., Cuddy, D. T., Daffer, W. H., Drouin, B. J., Fetzer, E., Froidevaux, L., Fuller, R., Herman, R., Jarnot, R. F., Jiang, J. H., Jiang, Y. B., Kelly, K., Knosp, B. W., Kovalenko, L. J., Livesey, N. J., Liu, H.-C., Manney, G.

L., Pickett, H. M., Pumphrey, H. C., Rosenlof, K. H., Sabounchi, X., Santee, M. L., Schwartz, M. J., Snyder, W. V., Stek, P. C., Su, H., Takacs, L. L., Thurstans, R. P., Vömel, H., Wagner, P. A., Waters, J. W., Webster, C. R., Weinstock, E. M., and Wu, D. L.: Aura Microwave Limb Sounder upper tropospheric and lower stratospheric H_2O and relative humidity with respect to ice validation, J. Geophys. Res. 112, D24S35, doi:10.1029/2007JD008752, 2007.

Read, W. G., Schwartz, M. J., Lambert, A., Su, H., Livesey, N. J., Daffer, W. H., and Boone, C. D.: The roles of convection, extratropical mixing, and in-situ freeze-drying in the Tropical Tropopause Layer, Atmos. Chem. Phys., 8, 6051–6067, 2008, http://www.atmos-chem-phys.net/8/6051/2008/.

Reid, G. C. and Gage, K. S.: The tropical tropopause over the western Pacific: Wave driving, convection, and the annual cycle, J. Geophys. Res., 101, 21233–21241, 1996.

Rosenfield, J. E., Considine, D. B., Schoeberl, M. R., and Browell, E. V.: The impact of subvisible cirrus clouds near the tropical tropopause on stratospheric water vapor, Geophys. Res. Lett., 25, 1883–1886, 1998.

Rosenlof, K. H.: Seasonal cycle of the residual mean meridional circulation in the stratosphere, J. Geophys. Res., 100(D3), 5173–5191, 1995.

Schwartz, M. J., Lambert, A., Manney, G. L., Read, W. G., Livesey, N. J., Froidevaux, L., Ao, C. O., Bernath, P. F., Boone, C. D., Cofield, R. E., Daffer, W. H., Drouin, B. J., Fetzer, E. J., Fuller, R. A., Jarnot, R. F., Jiang, J. H., Jiang, Y. B., Knosp, B. W., Krüger, K., Li, J.-L. F., Mlynczak, M. G., Pawson, S., Russell III, J. M., Santee, M. L., Snyder, W. V., Stek, P. C., Thurstans, R. P., Tompkins, A. M., Wagner, P. A., Walker, K. A., Waters, J. W., and Wu, D. L.: Validation of the Aura Microwave Limb Sounder temperature and geopotential height measurements, J. Geophys. Res., 113, D15S11, doi:10.1029/2007JD008783, 2008.

Sherwood, S. C.: A stratospheric "drain" over the maritime continent, Geophys. Res. Lett., 27, 677–680, 2000.

Sherwood, S. C. and Dessler, A. E.: A model for transport across the tropical tropopause, J. Atmos. Sci., 58, 765–779, 2001.

Sherwood, S. C., Horinouchi, T., and Zeleznik, H. A.: Convective impact on temperatures observed near the tropical tropopause, J. Atmos. Sci., 60, 1847–1856, 2003.

Sherwood, S. C., Chae, J. -H., Minnis, P., and McGill, M.: Underestimation of deep convective cloud tops by thermal imagery, Geophys. Res. Lett., 31, L11102, doi:10.1029/2004GL019699, 2004.

Smith, C. A., Haigh, J. D., and Toumi, R.: Radiative forcing due to trends in stratospheric water

vapour, Geophys. Res. Lett., 28, 179–182, 2001.
Stephens, G. L., Vane, D. G., Boain, R. J., Mace, G. G., Sassen, K., Wang, Z., Illingworth, A. J., O'Connor, E. J., Rossow, W. B., Durden, S. L., Miller, S. D., Austin, R. T., Benedetti, A., Mitrescu, C., and The CloudSat Science Team: The CloudSat and the A-Train, B. Am. Meteorol. Soc., 83, 1771–1790, 2002.
Tsuda, T., Ratnam, M. V., May, P. T., Alexander, M. J., Vincent, R. A., and MacKinnon, A.: Characteristics of gravity waves with short vertical wavelengths observed with radiosonde and GPS occultation during DAWEK (Darwin Area Wave Experiment), J. Geophys. Res., 109, D20S03, doi:10.1029/2004JD004946, 2004.
Webster, P. J. and Stephens, G. L.: Tropical upper-tropospheric extended clouds: Inferences from winter MONEX, J. Atmos. Sci., 37, 1521–1541, 1980.
Wu, D. L., Ackerman, S. A., Davies, R., Diner, D. J., Garay, M. J., Kahn, B. H., Maddux, B. C., Moroney, C. M., Stephens, G. L., Veefkind, J. P., and Vaughan, M. A.: Vertical distributions and relationships of cloud occurrence frequency as observed by MISR, AIRS, MODIS, OMI, CALIPSO, and CloudSat, Geophys. Res. Lett., 36, L09821, doi:10.1029/2009GL037464, 2009.
Wu, D. L., Chae, J. H., Lambert, A., and Zhang, F. F.: Characteristics of CALIOP attenuated backscatter noise: implication for cloud/aerosol detection, J. Geophys. Res., in review, 2010.
Yulaeva, E., Holton, J. R., and Wallace, J. M.: On the cause of the annual cycle in tropical lower-stratospheric temperatures, J. Atmos. Sci., 51(2), 169–174, 1994.
Zhou, X. L. and Holton, J. R.: Intraseasonal variations of tropical cold point temperatures, J. Climate, 15, 1460–1473, 2002.

ACPD
10, 8963–8994, 2010

ACPD

10, 8963–8994, 2010

The role of tropical deep convective clouds

J. H. Chae et al.

Title Page
Abstract Introduction
Conclusions References
Tables Figures
Back Close
Full Screen / Esc
Printer-friendly Version
Interactive Discussion

Table 1. MLS water vapor (Δq) and ozone (ΔO_3) anomalies above cloud top estimated by an adiabatic vertical displacement based on observed temperature anomalies ($\Delta\theta_{obs}$) at 15.6 km. Actual water vapor (Δq_{obs}) and ozone (ΔO_{3obs}) anomalies are also shown.

$\Delta\theta_{obs}$	$d\theta/dz$	dq/dz	Δq	Δq_{obs}	$\Delta O_3/dz$	ΔO_3	ΔO_{3obs}
1.494 K	13.487 K/km	−1.487 ppmv/km	−0.165 ppmv	−0.596 ppmv	17.347 ppbv/km	1.922 ppbv	3.400 ppbv

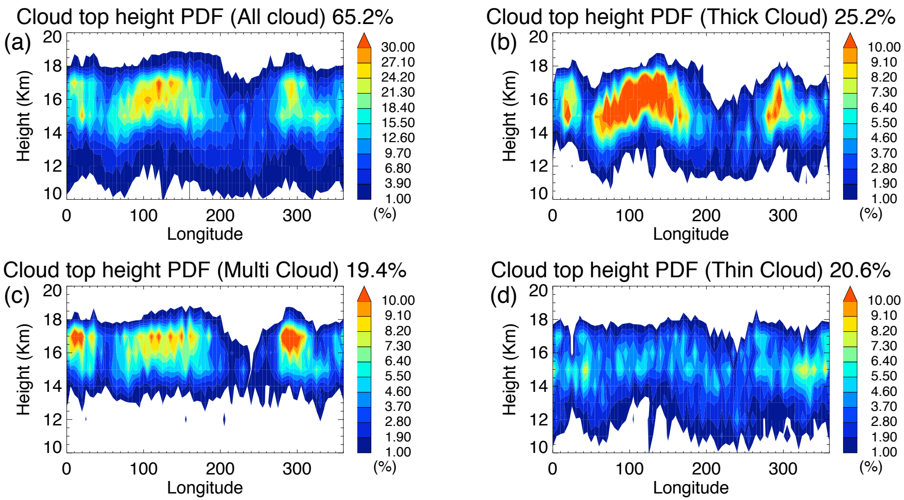

Fig. 1. Cloud top height frequency of 15° S–15° N with longitude for all clouds **(a)**, thick clouds (deep convection) **(b)**, multi-layered clouds **(c)**, and isolated thin clouds (thin cirrus clouds) **(d)**.

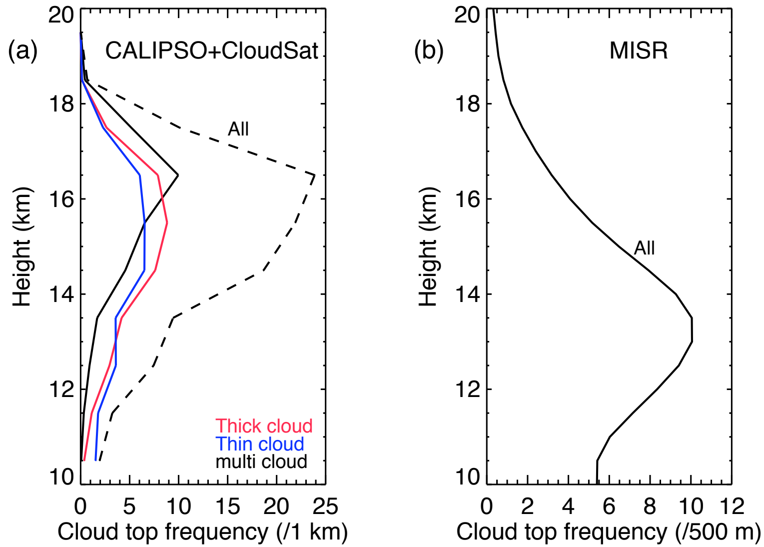

Fig. 2. Cloud top height frequency between 15° S–15° N from CALIPSO-CloudSat **(a)** and between 20° S–20° N from MISR **(b)**.

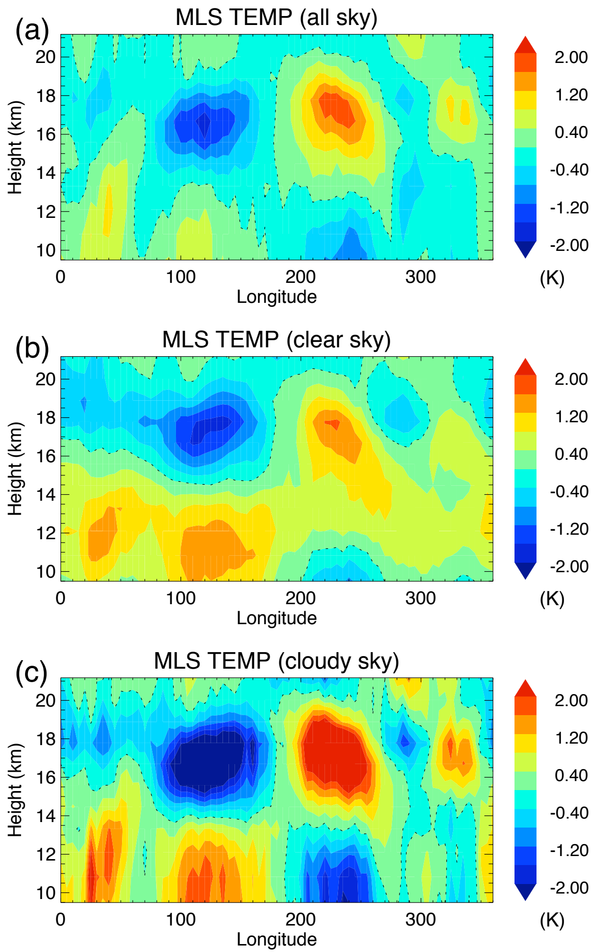

Fig. 3. Time mean zonal and vertical temperature anomalies from the zonal mean with removal of the annual cycle at each altitude.

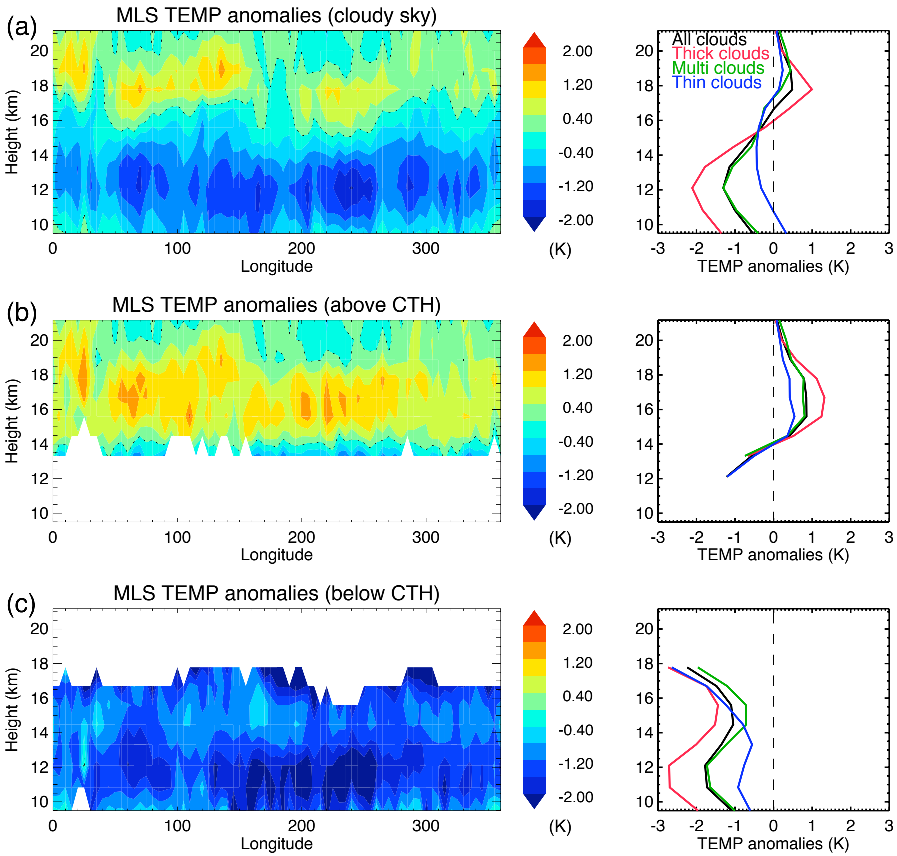

Fig. 4. Time mean longitudinal and vertical temperature anomalies from local clear sky mean temperature when for cloud tops over 10 km **(a)**. **(b)** the same as (a) except that each data height is at least 1.5 km higher than cloud top. **(c)** the same as (a) except data height is inside cloud but not lower than 3 km below cloud. Right figures show zonal averages with height.

ACPD
10, 8963–8994, 2010

Title Page
Abstract Introduction
Conclusions References
Tables Figures
◀| |▶
◀ ▶
Back Close
Full Screen / Esc
Printer-friendly Version
Interactive Discussion

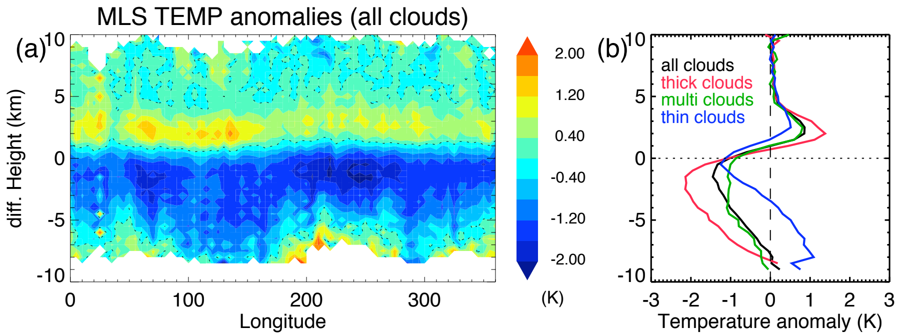

Fig. 5. Temperature anomalies relative to cloud top height versus longitude **(a)**, and zomally averaged for cloud types **(b)**.

ACPD
10, 8963–8994, 2010

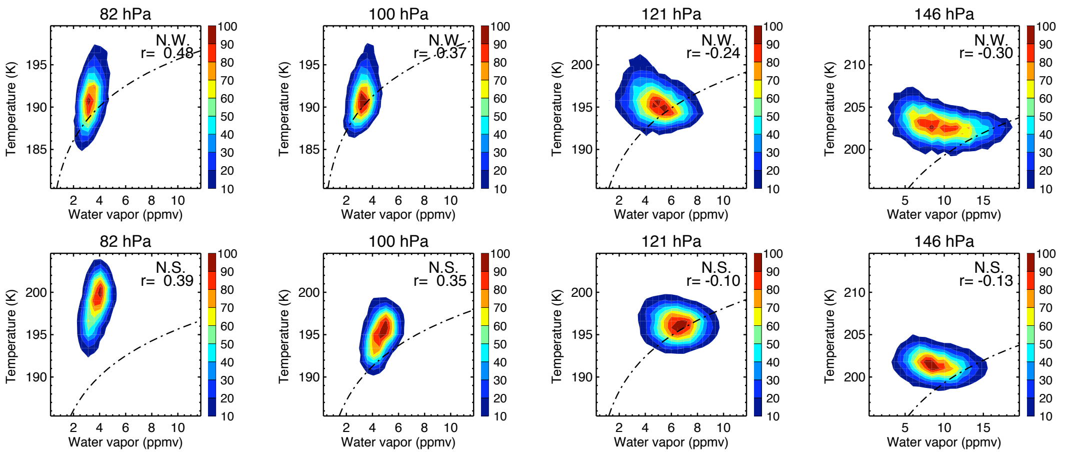

Fig. 6. The contour of temperature versus water vapor frequency from MLS. Dash-dot line shows the saturation line.

ACPD
10, 8963–8994, 2010

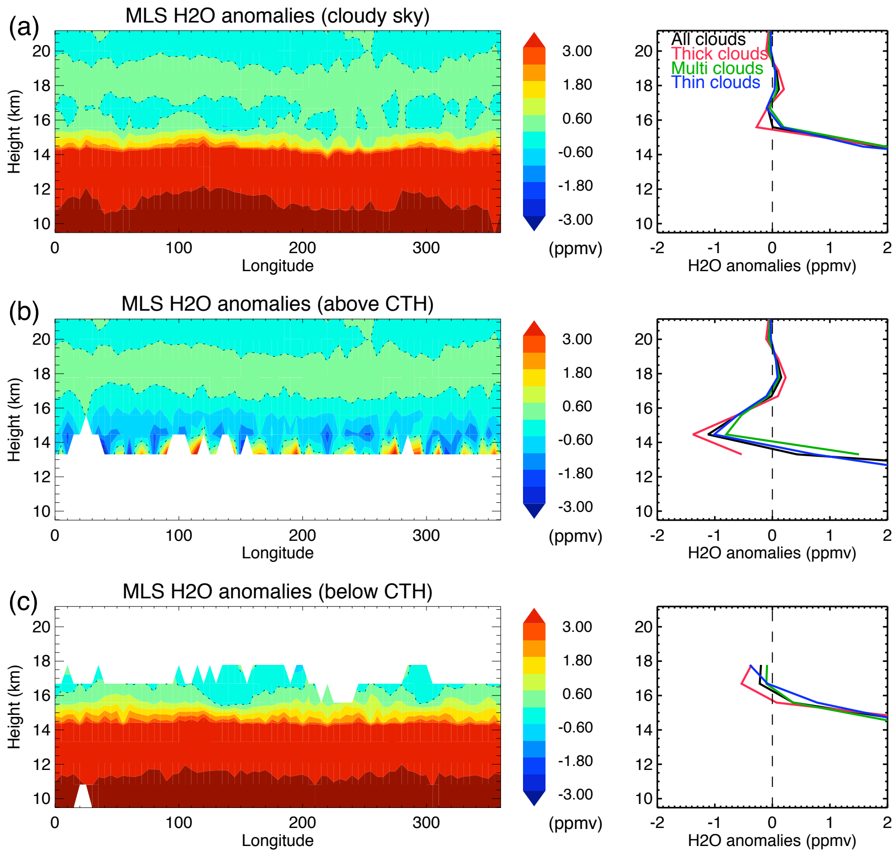

Fig. 7. The same as Fig. 4 except water vapor anomalies.

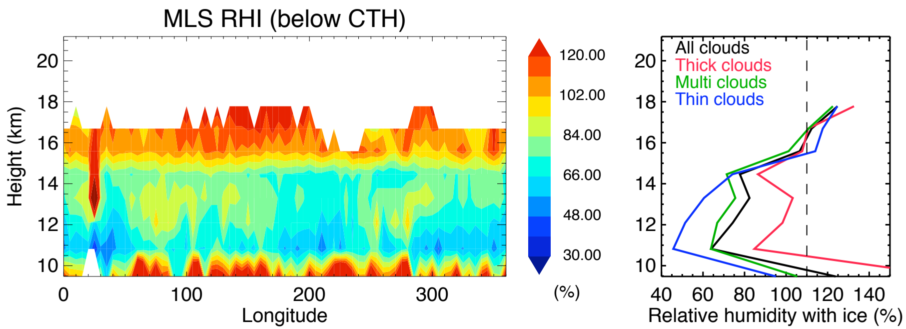

Fig. 8. Relative humidity with ice below cloud top height from MLS.

ACPD
10, 8963–8994, 2010

Title Page
Abstract
Introduction
Conclusions
References
Tables
Figures
◀
▶
Back
Close
Full Screen / Esc
Printer-friendly Version
Interactive Discussion

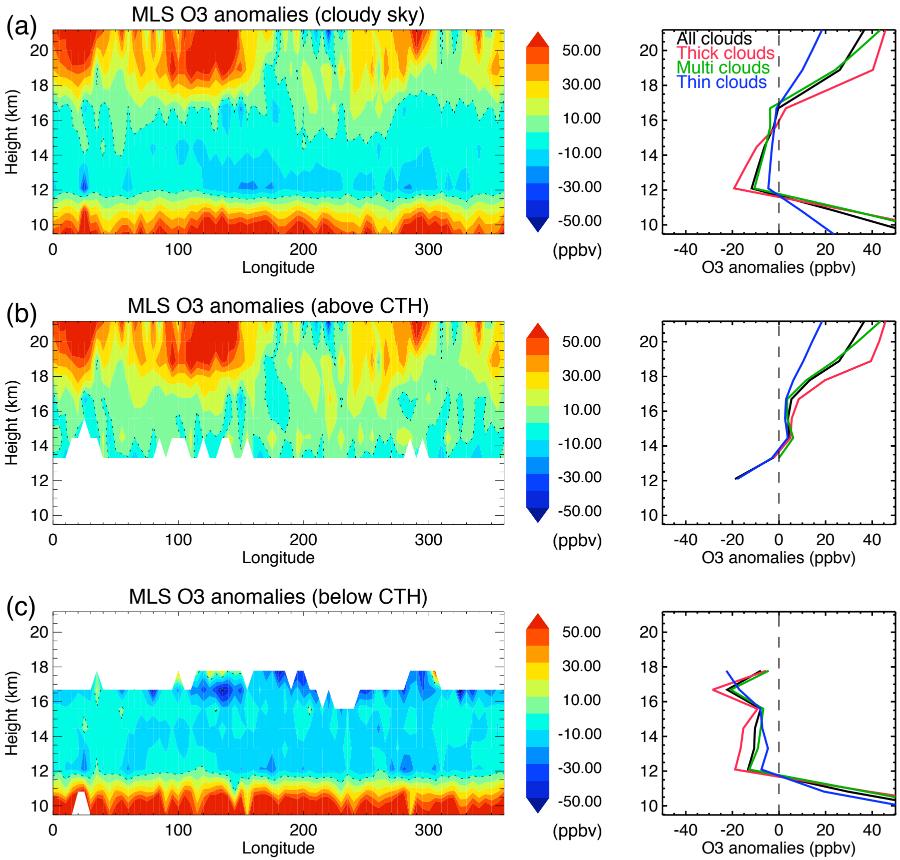

Fig. 9. The same as Fig. 4 except ozone anomalies.

ACPD
10, 8963–8994, 2010

The role of tropical deep convective clouds

J. H. Chae et al.

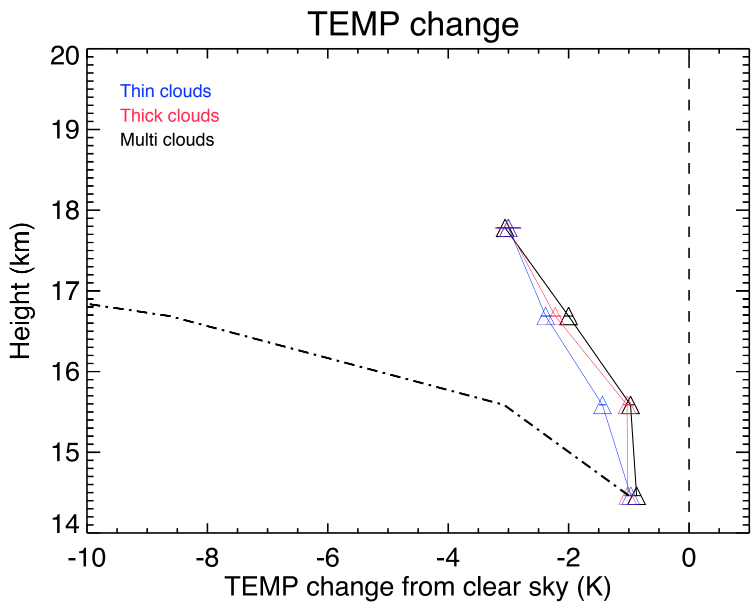

Fig. 10. Temperature anomalies near cloud top from zonal mean clear sky temperature. Dash-dot line shows idealized temperature anomalies without mixing with the environment when we assume that the LNB is 14.5 km.

ACPD
10, 8963–8994, 2010

The role of tropical deep convective clouds

J. H. Chae et al.

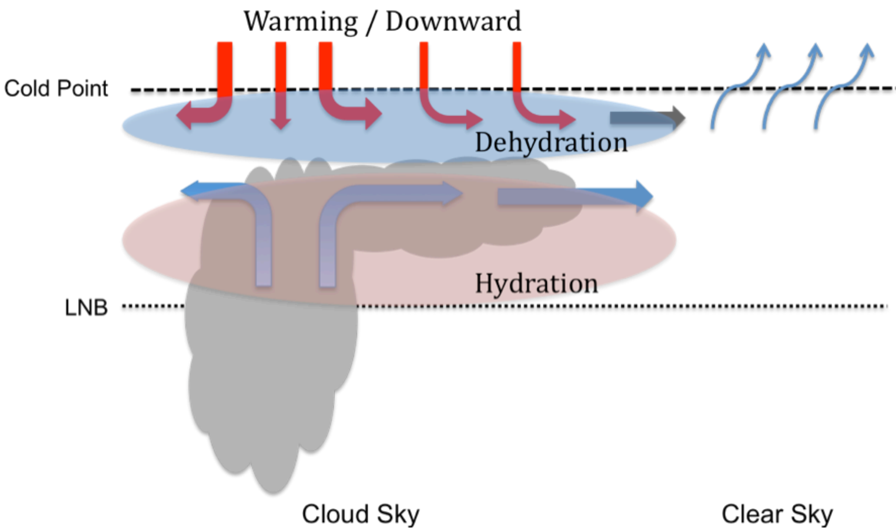

Fig. 11. A schematic of the dehydration process (including temperature variations) and water vapor transport to the stratosphere above cloud top in the TTL. Red color represents warming, and blue color represents cooling.

ACPD

10, 8963–8994, 2010

Title Page
Abstract Introduction
Conclusions References
Tables Figures
◀◀ ▶▶
◀ ▶
Back Close
Full Screen / Esc
Printer-friendly Version
Interactive Discussion